SEMARAK ILMU PUBLISHING
202103268166(003316878-P)

CFD Letters

Journal homepage:
https://semarakilmu.com.my/journals/index.php/CFD_Letters/index
ISSN: 2180-1363

Free Convection Boundary Layer Flow of Brinkman-Viscoelastic Fluid over a Horizontal Circular Cylinder with Constant Wall Temperature

Siti Farah Haryatie Mohd Kanafiah[1,2,*], Abdul Rahman Mohd Kasim[1,*♣], Syazwani Mohd Zokri[3], Nur Syamilah Arifin[4], Nur Syahidah Nordin[5], Masyfu'ah Mokhtar[5]

1 Universiti Malaysia Pahang, 26300 Kuantan, Pahang, Malaysia
2 Universiti Teknologi MARA Cawangan Kelantan, 18500 Machang, Kelantan, Malaysia
3 Universiti Teknologi MARA Cawangan Terengganu, 21080 Kuala Terengganu, Terengganu, Malaysia
4 Universiti Teknologi MARA Johor, 81570 Masai, Johor, Malaysia
5 Universiti Teknologi MARA Johor, 81300 Segamat, Johor, Malaysia

ARTICLE INFO

Article history:
Received 11 August 2022
Received in revised form 19 September 2022
Accepted 27 November 2022
Available online 12 January 2023

Keywords:
Free convection; Brinkman; viscoelastic; porosity; horizontal circular cylinder

ABSTRACT

The demand on the complex model on the study of fluid flow problem is crucial since the real fluid exist in industry applications cannot be presented by the conventional fluid anymore due to the complex properties of the materials. Since then, many mathematicians and scientist try to create the model that can be presented those fluids. Fluid which having characteristics viscous and elasticity can be categorized as non-Newtonian type of fluid due to its relations which against Newton's Law of viscosity. The application of the fluid is widespread in industrial applications including oils and gas sectors, the automobile industry and manufacturing processes. Paints is one of the examples of viscoelastic fluid since almost wall is painted by the materials polymer and solvents. Therefore, this work is intended to investigate the viscoelastic fluid flow with the porosity condition which then called as Brinkman-viscoelastic model. The flow is presumed to transfer over a geometry horizontal circular cylinder (HCC). The thermal boundary condition is set to be constant wall temperature (CWT). The governing equations which based on Navier Stokes equations are first transformed to the less complex form by utilizing a non-dimensionless and a non-similarity variable. The resulting equations were obtained in the partial differential equations (PDEs) and at the lower stagnation point case, the model is reduced to the ordinary differential equations (ODEs). The Keller-box method (KBM) is applied to solved the final equations. The validation process is performed by direct comparing with the established output in literature and found to be in a very strong agreement. This process is valid since the present model can be reduced to the previous model at the limiting case where the identical equations were obtained. The results of the present model are then computed and presented in tabular form and also illustrated in graphical form. It is noticed that the viscoelastic parameter and Brinkman Parameter significantly affected the fluid flow characteristics.

* *Corresponding author.*
E-mail address: sitif315@uitm.edu.my

♣ *Corresponding author.*
E-mail address: rahmanmohd@ump.edu.my

https://doi.org/10.37934/cfdl.15.1.103114

1. Introduction

Fluid dynamics, a component of fluid mechanics that explores the flow of fluids like liquids and gases, is an area of study in physics and engineering. Applications of fluid dynamics include determining the force and moment on an aeroplane, estimating the flow rate of petroleum mass through pipelines, understanding nebulae in interstellar space, and simulating fusion weapon blasts. Various fluid properties, including flow velocity, pressure, density, and temperature, are typically arranged as functions of space and time to solve a fluid dynamic problem.

Due to its numerous commercial and technological applications, particularly in manufacturing and processing, the study of non-Newtonian fluids has caught the attention of many academics. Because there is no single construction connection that can be used to explain all non-Newtonian fluids, they are more complex than Newtonian fluids [1]. Non-Newtonian fluids have a shear stress threshold before they begin to flow, can shear-thin or shear-thicken, be thixotropic, allow stress relaxation, creep in a nonlinear way, generate normal stress disparities, and more [2]. In describing the rheological properties of these fluids, several models have been derived such as the Power-law fluid, Ellis fluid, Casson fluid, Brinkman fluid, Carreu fluid, Bingham fluid, and viscoelastic fluid. Due to their wide range of applications, many researchers have studied the flow of non-Newtonian fluids, particularly when dealing with porous media condition. The Brinkman model is a well-known model for porous media that can be applied to surfaces with significant porosity or incompressible fluid flow. The fluid with a viscosity and elasticity feature is one of the most typical non-Newtonian fluids to consider. There are several previous literatures had focused on Brinkman and viscoelastic model as mentioned in [3 -8].

The free convection in a porous medium problem is one that is frequently studied in a variety of geometries, boundary conditions, and fluid types in the context of heat transfer and fluid flow problems. Mohamed, *et al.* [9] found that skin friction encountered significant friction in the centre of the cylinder surface while the Nusselt number exhibits a diminishing fluctuation in their investigation of fluid flow through HCC. They came to the conclusion that the component surface is harmed by the high friction between the fluid and the cylinder. The local heat transmission at the cylinder surface is significantly enhanced by lowering the Dufour number while simultaneously raising the Soret number, according to Vasu *et al.* [10]. Recently, several authors [11–13] studies concentrated using the CWT on non-Newtonian fluids in porous media.

The boundary layer flow of a non-Newtonian fluid in a porous region had been discussed in earlier publications. The aim of this paper is to explore the free convective boundary layer flow of a Brinkman-viscoelastic fluid moving through HCC with CWT, which is motivated by earlier studies by Nazar *et al.* [3] and Mahat *et al.* [7]. It is examined how Brinkman and the viscoelastic parameter affect the speed, temperature, skin friction coefficient, and Nusselt number. The non-dimensional variables and non-similarity transformations are used to convert the complex into dimensionless PDEs. For numerical computations, KBM is employed in the computational MATLAB R2019a software. The graphs are plotted to show the behaviors of physical variables.

2. Methodology

This study starts with mathematical formulation of the basic governing equations by using the boundary layer approximations. The non-linear dimensionless PDEs is obtained by utilizing the non-dimensional and non-similarity variables. The four steps of KBM are applied to solve the PDEs numerically with the help of MATLAB algorithm. Finally, the results are validated and analysed in graphical form.

2.1 Mathematical Formulation

Consider a free convection flow past a HCC of radius a placed in a porous region as illustrated in Figure 1. In the case of free convection, the external velocity can be ignored because the velocity external to the boundary layer is simply the absorption velocity owing to pressure motion, not the induced free stream velocity. The ambient temperature and CWT are respectively defined as T_∞ and T_w. The coordinate of $\bar{x}$ is measured around the cylinder and and $\bar{y}$ is perpendicular to the surface, respectively.

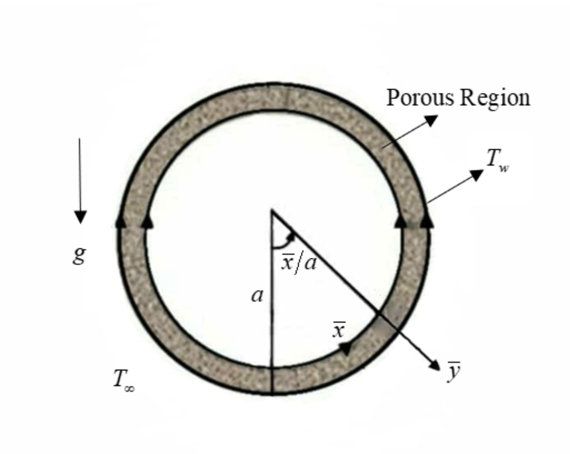

Fig. 1. Two-dimensional geometry of the flow

The basic governance equations of Brinkman fluid consist of continuity, momentum and energy equations. According to Guta and Sundar [14] and Nield and Bejan [15], the equations of an incompressible fluid in vectorial form are written as

$$\nabla \cdot \rho \mathbf{V} = 0, \tag{1}$$

$$\frac{\mu}{K}\mathbf{V} = -\nabla p + \nabla.\boldsymbol{\tau} + F_b, \tag{2}$$

$$\mathbf{V} \cdot \nabla T = \alpha_m \nabla^2 T, \tag{3}$$

where the operator $\nabla = \left\langle \frac{\partial}{\partial \bar{x}}, \frac{\partial}{\partial \bar{y}}, \frac{\partial}{\partial \bar{z}} \right\rangle$ is defined as vector operator, $\mathbf{V} = \langle \bar{u}, \bar{v}, \bar{w} \rangle$ is velocity vector, μ is dynamic viscosity, K is permeability of porous media, p is pressure, $\boldsymbol{\tau}$ is stress tensor, F_b is the body force and T is the fluid temperature.

Employing the Brinkman model to the viscoelastic model, an additional viscoelastic term is incorporated in momentum equation to describe the fluid viscosity and elasticity. The modified Cauchy stress tensor for Brinkman-viscoelastic fluid based on Tonekaboni *et al.,* [16] and Guta and Sundar [14] is

$$\boldsymbol{\tau} = -\bar{p}\mathbf{I} + 2\frac{\mu}{\phi}\mathbf{d} + 2k_0 \overset{\nabla}{\mathbf{d}} \tag{4}$$

that represent the constitutive equation of Brinkman-viscoelastic fluid. Here, $\mathbf{I},\mathbf{d},\overset{\nabla}{\mathbf{d}},\phi$ and k_0 are declared as identity tensor, deformation rate tensor, upper-convected derivative, porosity of porous region and the short-memory coefficient, respectively. Note that, the variable upper-convected derivative of tensor is defined as

$$\overset{\nabla}{\mathbf{d}} = \left(\mathbf{V}\cdot\nabla\right)\mathbf{d} - \mathbf{d}\cdot\left(\nabla\mathbf{V}\right)^{tr} - \nabla\mathbf{V}\cdot\mathbf{d} \tag{5}$$

Hence, using the constitutive eq. (4), the set of governing equations are obtained by applying the boundary layer assumptions as follow

$$\frac{\partial\bar{u}}{\partial\bar{x}} + \frac{\partial\bar{v}}{\partial\bar{y}} = 0 \tag{6}$$

$$\begin{aligned}\frac{\mu}{K}\,\bar{u} = \frac{\mu}{\phi}\frac{\partial^2\bar{u}}{\partial\bar{y}^2} &+ k_0\left[\bar{u}\,\frac{\partial^3\bar{u}}{\partial\bar{x}\partial\bar{y}^2} + \bar{v}\,\frac{\partial^3\bar{u}}{\partial\bar{y}^3} - \frac{\partial\bar{u}}{\partial\bar{y}}\frac{\partial^2\bar{u}}{\partial\bar{x}\partial\bar{y}} + \frac{\partial\bar{u}}{\partial\bar{x}}\frac{\partial^2\bar{u}}{\partial\bar{y}^2}\right]\\ &+\rho_\infty g\beta\left(T - T_\infty\right)\sin\left(\frac{\bar{x}}{a}\right)\end{aligned} \tag{7}$$

$$\bar{u}\,\frac{\partial T}{\partial\bar{x}} + \bar{v}\,\frac{\partial T}{\partial\bar{y}} = \alpha_m\,\frac{\partial^2 T}{\partial\bar{y}^2} \tag{8}$$

together with appropriate boundary conditions for CWT

$$\begin{aligned}&\bar{v} = 0,\quad \bar{u} = 0,\quad T = T_w \quad \text{at } \bar{y} = 0\\ &\bar{u} \to 0,\quad \bar{v} \to 0,\quad T \to T_\infty \quad \text{as } \bar{y} \to \infty\end{aligned} \tag{9}$$

2.1.1 Non-dimensional Variables

According to Chamkha *et al.* [17], the non-dimensional variables applied to the Eqs. (6) to (9) are introduced as follows

$$x = \bar{x}/a,\quad y = Ra^{1/2}(\bar{y}/a),\quad u = \frac{\bar{u}}{U_c},\quad v = Ra^{1/2}\,\frac{\bar{v}}{U_c},\theta = (T - T_\infty)/(T_w - T_\infty) \tag{10}$$

where $Ra = \dfrac{\rho_\infty gk\beta\left(T_w - T_\infty\right)a}{\alpha_m\mu}$ is the Rayleigh number and $U_c = \dfrac{\rho_\infty gk\beta\left(T_w - T_\infty\right)}{\mu}$ is the characteristic velocity. Then, the dimensionless PDEs yield to

$$\frac{\partial u}{\partial x} + \frac{\partial v}{\partial y} = 0 \tag{11}$$

$$\frac{\partial u}{\partial y}=\Gamma\frac{\partial^3 u}{\partial y^3}+k_1\begin{bmatrix} u\dfrac{\partial^4 u}{\partial x\partial y^3}+\dfrac{\partial^3 u}{\partial x\partial y^2}\dfrac{\partial u}{\partial y}+v\dfrac{\partial^4 u}{\partial y^4}+\dfrac{\partial^3 u}{\partial y^3}\dfrac{\partial v}{\partial y} \\ -\dfrac{\partial u}{\partial y}\dfrac{\partial^3 u}{\partial x\partial y^2}-\dfrac{\partial^2 u}{\partial x\partial y}\dfrac{\partial^2 u}{\partial y^2} \\ +\dfrac{\partial u}{\partial x}\dfrac{\partial^3 u}{\partial y^3}+\dfrac{\partial^2 u}{\partial y^2}\dfrac{\partial^2 u}{\partial x\partial y} \end{bmatrix}+\frac{\partial \theta}{\partial y}\sin x \tag{12}$$

$$u\frac{\partial \theta}{\partial x}+v\frac{\partial \theta}{\partial y}=\frac{\partial^2 \theta}{\partial y^2} \tag{13}$$

together with the boundary conditions

$$\begin{aligned} &u=0,\quad v=0,\quad \theta=1 \quad \text{at } y=0 \\ &u\to 0,\quad v\to 0,\quad \theta\to 0 \quad \text{as } y\to\infty \end{aligned} \tag{14}$$

2.1.1 Non-similarity Transformation

Then, the non-similarity transformation is introduced to find the solutions of Eqs. (11) to (14) as below

$$\psi = x\,f(x,y),\ \theta=\theta(x,y),\ u=\frac{\partial \psi}{\partial y},\ v=-\frac{\partial \psi}{\partial x} \tag{15}$$

The Eq. (11) is automatically satisfied using the above equations and Eqs. (12) and (13) are as follows

$$f'-\Gamma f'''-k_1\left[2f'f'''-ff^{(iv)}-\left(f''\right)^2\right]-\theta\frac{\sin x}{x}=xk_1\left[f'\frac{\partial f'''}{\partial x}-\frac{\partial f}{\partial x}f^{(iv)}-f''\frac{\partial f''}{\partial x}^2+\frac{\partial f'}{\partial x}f'''\right] \tag{16}$$

$$\theta''+f\,\theta'=x\left(f'\frac{\partial \theta}{\partial x}-\frac{\partial f}{\partial x}\theta'\right) \tag{17}$$

and the boundary conditions (14) become

$$\begin{aligned} &f(0)=0,\quad f'(0)=0,\quad \theta(0)=1, \\ &f'(\infty)\to 0,\quad f''(\infty)\to 0,\quad \theta(\infty)\to 0 \end{aligned} \tag{18}$$

The PDEs (16) to (17) are transformed to the ODEs form at $x\approx 0$,

$$f'-\Gamma f'''-k_1\left[2f'f'''-ff^{(iv)}-\left(f''\right)^2\right]-\theta=0 \tag{19}$$

$$\theta''+f\,\theta'=0 \tag{20}$$

subjected to the boundary condition (18).

By imposing the coefficient of skin friction and local Nusselt number by Kanafiah *et al.* [18], it can be written as

$$C_f Ra^{1/2} / \Pr = x \frac{\partial^2 f}{\partial y^2}, \quad Nu_x Ra^{-1/2} = -\frac{\partial \theta}{\partial y}. \tag{21}$$

2.2 Numerical Method

KBM is used in this study to obtain the numerical results of Eqs. (16) and (17). The main sources for this method are presented in the works by Kanafiah *et al.* [18] which include the four steps of KBM:1. Reduce the non-linear PDEs to first order system, 2. Write in the finite difference form using central difference, 3. Linearize the system using Newton's method, and 4. Solved by using block tridiagonal elimination technique. The numerical algorithms and computation are performed in the MATLAB R2019a software. The computations are done by selecting the finite boundary layer thickness within $7 \le y_\infty \le 12$ and step size, $\Delta y = 0.02$. The various Brinkman and viscoelastic parameters are computed to determine the fluid flow velocity and temperature profile, the coefficient of local skin friction and Nusselt number. The numerical analysis is summarised in graphical form.

3. Results and Discussions

The present findings are compared with numerical solution of Nazar *et al.* [3] in the exclusion of k_1 with the added constant A in Eqn. (19). Table 1 shows the current model at stagnation point which is compared to the existing equation with a few limited cases. The comparing values for $f''(0)$ and $-\theta'(0)$ are also validated with the previous literature as display in Table 2 which is indicated that the current results are in strong connection to the previous values, thereby numerical algorithm proposed in this research are considered to be precise.

Table 1
Comparative model at lower stagnation point

Author	Model	Limiting cases
Current	$f' - \Gamma f''' - k_1\left[2f'f''' - ff^{(iv)} - (f'')^2\right] - A - \theta = 0$	$k_1 = 0, A = 1$
Nazar *et al.* [3]	$f' - \Gamma f''' - A - \lambda\theta = 0$	$A = 1, \lambda = 1$

Table 2
Comparative values of $f''(0)$ and $-\theta'(0)$ with $A = 1$, $k_1 = 0$, $\lambda = 1$ and various Γ

Γ	Nazar *et al.* [3]		Current	
	$f''(0)$	$-\theta'(0)$	$f''(0)$	$-\theta'(0)$
0	-	1.0191	-	1.0190
0.1	5.5923	0.7791	5.5922	0.7790
0.2	3.8173	0.7251	3.8173	0.7249
0.3	3.0457	0.6919	3.0436	0.6938

Figures 2 to 5 illustrate the behaviour of velocity and temperature distributions as the value of k_1 and Γ rises. It is clear from Figure 2 that the impact of k_1 brings about the reduction of velocity about $y=0$ to 3, followed by the reversal trend of velocity profile where it increases in the direction of free stream. This circumstance is associated with dual physical properties of viscoelastic named viscous and elastic that aids to resist the fluid motion. For that reason, the incremented temperature profile illustrated through Figure 3 is anticipated owing to the convection process. Figure 4 behaves oppositely from that of Figure 2 where a decreasing trend of fluid flow is observed approximately about $y=2.5$, and then the graph flips over to cause an escalation in fluid flow when Γ increases from 0.1 to 0.7. Such outcome arises due to the impact of drag force which subsequently results in the slight increase of thermal boundary layer thickness.

Next, Figures 6 – 9 portray the natural propensity of physical quantities $C_f Pe^{1/2}/\Pr$ and $NuPe^{-1/2}$ in response to the variations of k_1 and Γ, respectively. It can be noticed that, an enhancement in $C_f Pe^{1/2}/\Pr$ is accompanied by the influences of both parameters while $NuPe^{-1/2}$ experiences reducing behaviour. Other than that, at the particular value of x, the performance of all quantities deteriorates with increasing value of involved parameters. This observation accords with our earlier findings which revealed that the acceleration in velocity and temperature profiles is due entirely to the increment effects in each parameter. Therefore, the friction and heat transfer rate at the surface are reduced. Note that, both quantities are indeed worthy of investigation on account that they displayed the behaviour of fluid flow on the geometry surface which can be useful in designing the wall of devices in engineering applications.

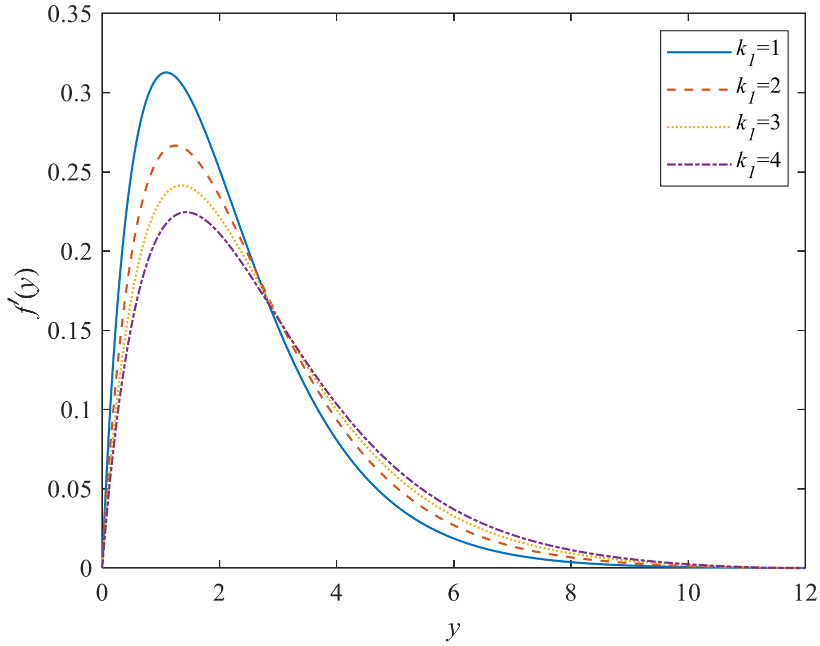

Fig. 2. Variation of $f'(y)$ for various k_1

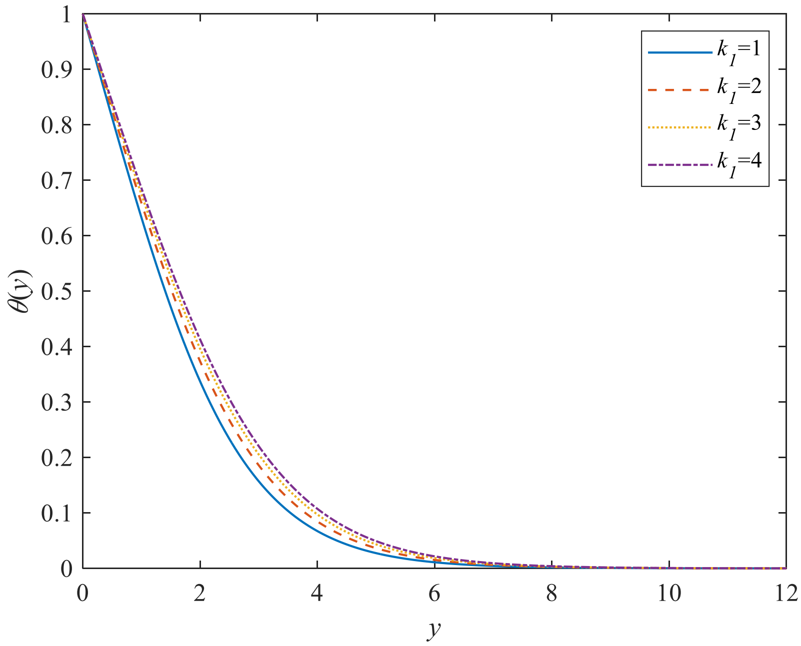

Fig. 3. Variation of $\theta(y)$ for various k_1

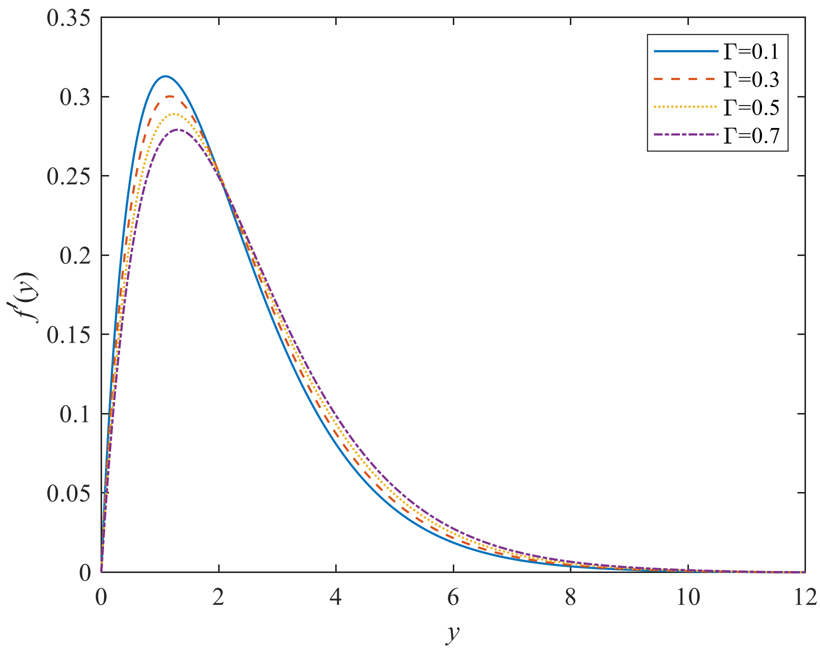

Fig. 4. Variation of $f'(y)$ for various Γ

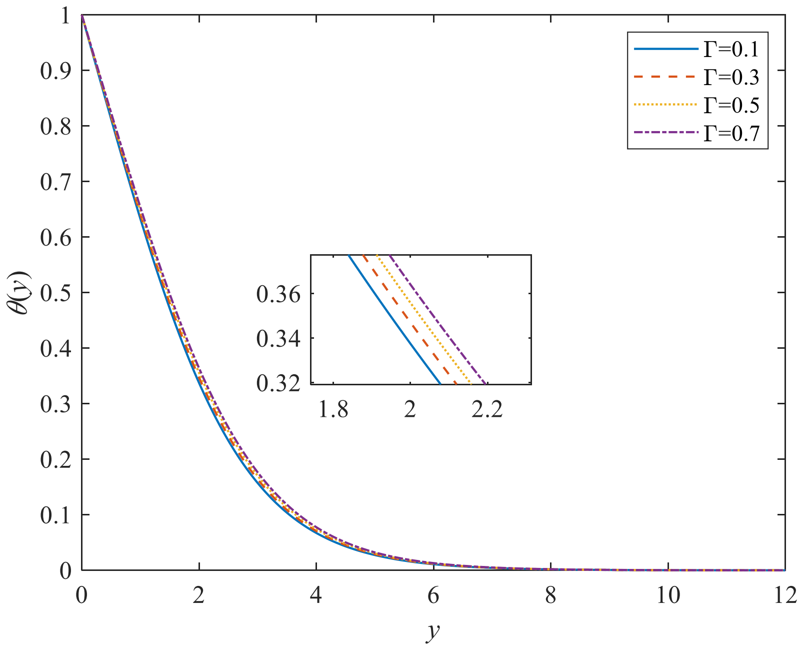

Fig. 5. Variation of $\theta(y)$ for various Γ

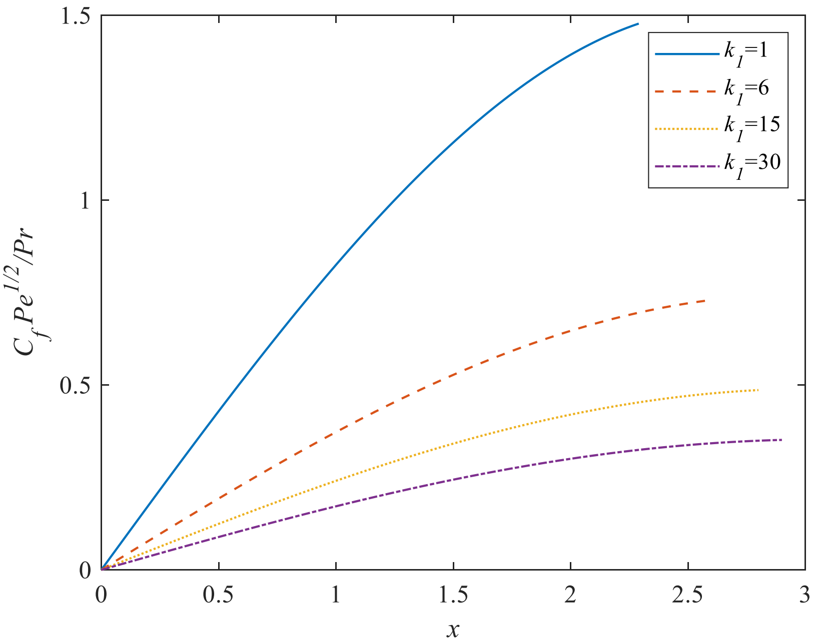

Fig. 6. Performance of $C_f Pe^{1/2} / \mathrm{Pr}$ for various k_1

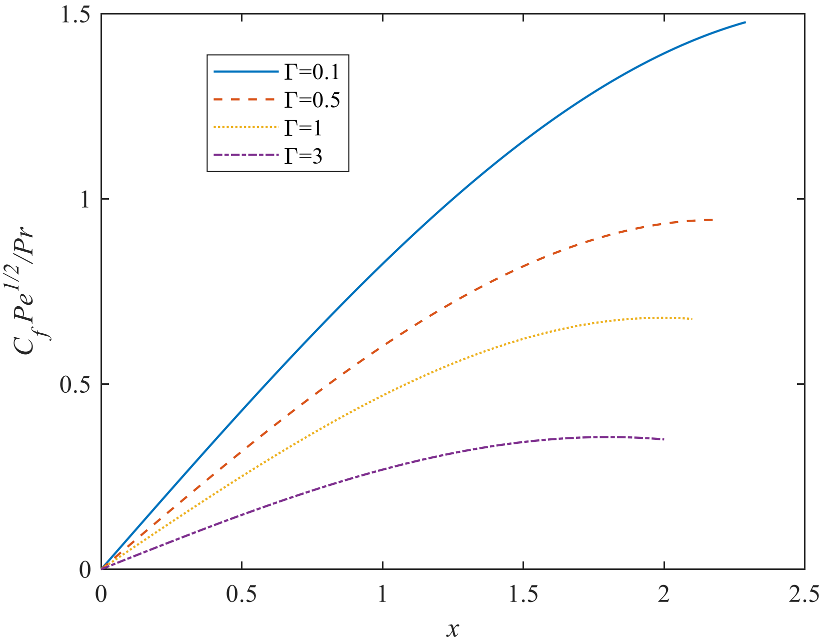

Fig. 7. Performance of $C_f Pe^{1/2}/\Pr$ for various Γ

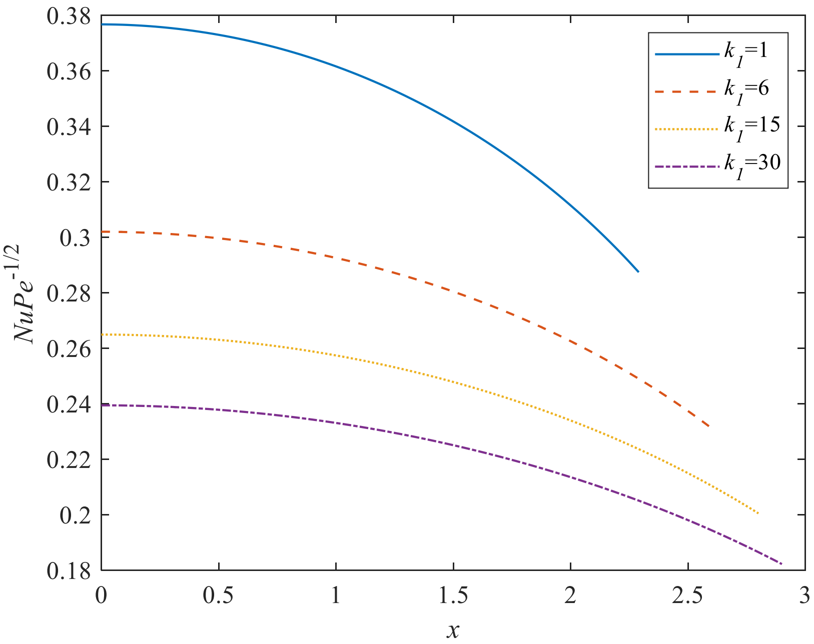

Fig. 8. Performance of $NuPe^{-1/2}$ for various k_1

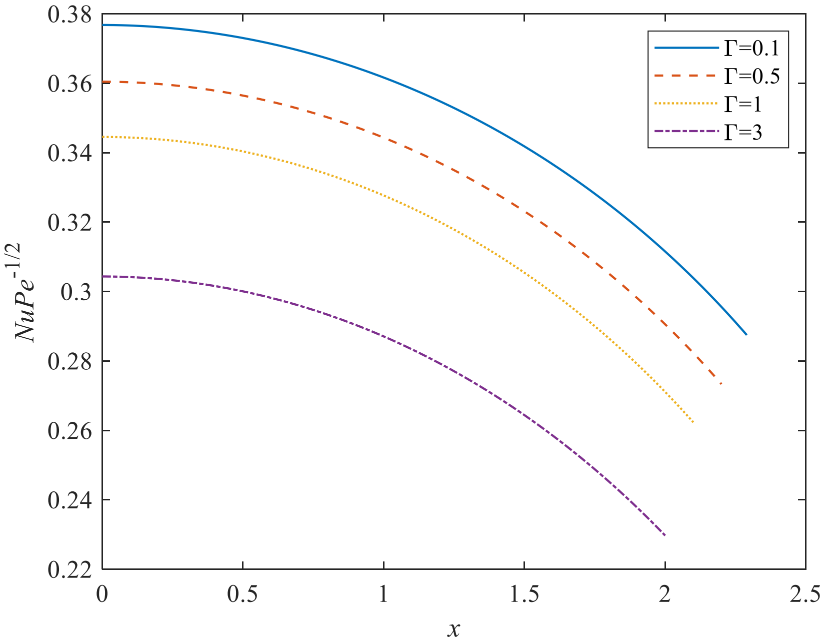

Fig. 9. Performance of $NuPe^{-1/2}$ for various Γ

4. Conclusions

This study has deliberated investigations on two-dimensional free convection of non-Newtonian fluid. It is caters the Brinkman-viscoelastic fluid model passing over HCC. The process of mathematical formulation and numerical method are explained in detail in the respective section 2.1 and 2.2. This research has explored quite evidently the effect of several parameters towards the flow field behavior and heat transfer features such as velocity and temperature distribution, the coefficient of skin friction and Nusselt number. As a whole, the outcome to emerge from this exploration are:

i. The viscoelastic fluid parameter, k_1 shows contradict behavior for the velocity and temperature distribution starting from $y=0$ to 3. Increasing k_1 has reduced the velocity of the fluid within $0 \le y \le 3$ while increased the temperature.
ii. The Brinkman parameter, Γ also shows the similar trend as k_1. The fluid velocity decreased until $y=2.5$ while temperature behaves oppositely as Γ increased.
iii. The increase of both parameters, k_1 and Γ has shown the similar behavior of skin friction coefficient and Nusselt number.

Acknowledgement
The authors would like to thank Universiti Malaysia Pahang for financial support through RDU213204 and Universiti Teknologi MARA Kelantan, Universiti Teknologi MARA Johor, Universiti Teknologi MARA Terengganu for their assistance and support.

References
[1] Kahshan, Muhammad, Dianchen Lu, and Mohammad Rahimi-Gorji. "Hydrodynamical study of flow in a permeable channel: Application to flat plate dialyzer". *International Journal of Hydrogen Energy* 44 (2019): 17041–17047. https://doi.org/10.1016/j.ijhydene.2019.04.211

[2] Shateyi, Stanford, and Hillary Muzara. “On the Numerical Analysis of Unsteady MHD Boundary Layer Flow of Williamson Fluid Over a Stretching Sheet and Heat and Mass Transfers.” *Computation* 8 (2020): 55. https://doi.org/10.3390/computation8020055

[3] Nazar, R.; Amin, N.; Filip, D.; Pop, I. The Brinkman model for the mixed convection boundary layer flow past a horizontal circular cylinder in a porous medium. *Int. J. Heat Mass Transf.* 46 (2003): 3167–3178. https://doi.org/10.1016/S0017-9310(03)00122-4

[4] Shafie, S.; Saqib, M.; Khan, I.; Qushairi, A. Mixed Convection Flow of Brinkman Type Hybrid Nanofluid Based on Atangana-Baleanu Fractional Model. *J. Phys. Conf. Ser.* 1366 (2019): 012041. http://dx.doi.org/10.1088/1742-6596/1366/1/012041

[5] Kanafiah, Siti Farah Haryatie Mohd, Abdul Rahman Mohd Kasim, Syazwani Mohd Zokri, and Hussien Ali Muhammed Al Sharifi. "Mixed convection flow of Brinkman fluid with convective boundary condition at lower stagnation point of horizontal circular cylinder." *Data Analytics and Applied Mathematics (DAAM)* 2, no. 1 (2021): 01-10. https://doi.org/10.15282/daam.v2i1.6310

[6] Khashi'ie, N.S., Waini, I., Zokri, S.M., Kasim, A.R.M., Arifin, N.M. and Pop, I., "Stagnation point flow of a second-grade hybrid nanofluid induced by a Riga plate", *International Journal of Numerical Methods for Heat & Fluid Flow* 32 No. 7 (2022): 2221-2239. https://doi.org/10.1108/HFF-08-2021-0534

[7] Mahat, Rahimah, Noraihan Afiqah Rawi, Abdul Rahman Mohd Kasim, and Sharidan Shafie. "Heat generation effect on mixed convection flow of viscoelastic nanofluid: convective boundary condition solution." *Malaysian Journal of Fundamental and Applied Sciences* 16, no. 2 (2020): 166-172. https://doi.org/10.11113/mjfas.v16n2.1367

[8] Ewis, Karem Mahmoud. “Effects of Variable Thermal Conductivity and Grashof Number on Non-Darcian Natural Convection Flow of Viscoelastic Fluids With Non Linear Radiation and Dissipations”. *Journal of Advanced Research in Applied Sciences and Engineering Technology* 22 (2021):69-80. https://doi.org/10.37934/araset.22.1.6980

[9] Mohamed, Muhammad Khairul Anuar, Mohd Zuki Salleh, Fadhilah Che Jamil, Ong Huie Ruey. “Free convection boundary layer flow over a horizontal circular cylinder in Al2O3-Ag/water hybrid nanofluid with viscous dissipation.” *Malaysian Journal of Fundamental and Applied Sciences* 17, no. 1 (2021): 20-25. https://doi.org/10.11113/mjfas.v17n1.1964

[10] Vasu, B., Rama Subba Reddy Gorla, P.V.S.N. Murthy, V.R. Prasad, O.A. Bég and S. Siddiqa. “MHD Free Convection-Radiation Interaction in a Porous Medium-Part II: Soret/Dufour Effects.” International Journal of Applied Mechanics and Engineering, no. 25 (2) (2020): 157-175. https://doi.org/10.2478/ijame-2020-0027

[11] Nirwana Japili, Haliza Rosali, and Norfifah Bachok. “Slip Effect on Stagnation Point Flow and Heat Transfer Over a Shrinking/Stretching Sheet in A Porous Medium With Suction/Injection”. *Journal of Advanced Research in Fluid Mechanics and Thermal Sciences* 90, no. 2 (2022): 73-89. http://doi.org/10.37934/arfmts.90.2.7389

[12] Huang, Chuo-Jeng and Kuo-Ann Yih. “Nonlinear Radiation and Variable Viscosity Effects on Free Convection of a Power-Law Nanofluid Over a Truncated Cone in Porous Media with Zero Nanoparticles Flux and Internal Heat Generation.” *Journal of Thermal Science and Engineering Applications* 13, 031020-1 (2021). https://doi.org/10.1115/1.4048453

[13] Mohd Kanafiah, Siti Farah Haryatie, Abdul Rahman Mohd Kasim, Syazwani Mohd Zokri, and Mohd Rijal Ilias. “Combined Convective Transport of Brinkman-Viscoelastic Fluid Across Horizontal Circular Cylinder With Convective Boundary Condition”. *Journal of Advanced Research in Fluid Mechanics and Thermal Sciences* 89, no. 2 (2022):15-24. http://doi.org/10.37934/arfmts.89.2.1524

[14] Guta, Lemi, and S. Sundar. “Navier-Stokes-Brinkman System for Interaction of Viscous Waves With a Submerged Porous Structure”. *Tamkang Journal of Mathematics* 41, no. 3 (2010): 217-43. https://doi.org/10.5556/j.tkjm.41.2010.722

[15] Nield, D. A., and Bejan, A. (2017). *Convection in Porous Media*, Springer, New York.

[16] Tonekaboni, S. A.; Abkar, R.; Khoeilar, R. On the Study of Viscoelastic Walters’ B Fluid in Boundary Layer Flows. *Mathematical Problems in Engineering* 2012 (2012): 1–18. https://doi.org/10.1155/2012/861508

[17] A.J. Chamkha, C. Bercea and I. Pop, Free convection from a vertical cylinder embedded in a porous medium filled with cold water, *Int. J. of Applied Mechanics and Engineering* 9, No.2 (2004): 273-283.

[18] Mohd Kanafiah, Siti Farah Haryatie, Abdul Rahman Mohd Kasim, Syazwani Mohd Zokri, Sharidan Shafie, Numerical solutions of convective transport on Brinkman-viscoelastic fluid over a bluff body saturated in porous region, *Case Studies in Thermal Engineering* 28 (2021): 101341, https://doi.org/10.1016/j.csite.2021.101341